

Estimation of Boreal Forest Properties From TanDEM-X Data Using Inversion of the Interferometric Water Cloud Model

Maciej J. Soja, *Member, IEEE*, Jan I. H. Askne, *Life Fellow, IEEE*, and Lars M. H. Ulander, *Fellow, IEEE*

Abstract—In this letter, the interferometric water cloud model (IWCM) is fit to 87 VV-polarized TanDEM-X acquisitions made between June 2011 and August 2014 over a boreal forest in Krycklan, northern Sweden, using a new method based on nonlinear least-squares optimization. A high-resolution digital terrain model is used as ground reference during interferometric synthetic-aperture radar (InSAR) processing and 26 stands with areas 1.5–22 ha and unaltered during the study period are studied. The dependence of biomass estimation performance, ground and vegetation backscatter coefficients (σ_{gr}^0 and σ_{veg}^0), canopy attenuation (α), and zero-biomass coherence (γ_0) on selected system and environmental parameters is studied. High correlation between the estimated biomass and reference biomass derived from *in situ* measurements is observed for all 87 acquisitions (r between 0.81 and 0.93), while the root-mean-square difference is between 18% and 32% for all 43 acquisitions made in snow-free conditions and with heights-of-ambiguity (HOAs) between 36 and 150 m. Significant biomass estimation bias is observed for HOAs above 150 m and for some acquisitions over snow-covered forest. It is also observed that σ_{gr}^0 and σ_{veg}^0 are the largest for temperatures below 0 °C and with significant snow cover. For temperatures above 0 °C, σ_{gr}^0 appears independent of temperature, while σ_{veg}^0 shows a tendency to increase with temperature. Moreover, γ_0 decreases from just below 1 for HOAs around 40 m to around 0.8 for HOAs above 150 m.

Index Terms—Above-ground biomass (AGB), boreal forest, interferometric model inversion, interferometric synthetic-aperture radar (InSAR), TanDEM-X.

I. INTRODUCTION

DUE to its high spatial resolution and good sensitivity to the vertical structure, interferometric synthetic-aperture radar (InSAR) has the potential to become an important tool for mapping and monitoring of above-ground dry biomass (AGB), which is a forest parameter important for climate modeling [1]. However, the relation between interferometric observables and biomass is nontrivial, mainly due to an ill-posed problem and difficulties in finding simple yet general scattering models. In order to be able to extract valuable information from InSAR data, scattering from forests must

be understood and the dependence of InSAR observables on biomass, environmental factors, and InSAR system configuration must be modeled.

During the past decades, several different interferometric models have been proposed and used [2]–[6]. One of the oldest and most flexible interferometric models is the interferometric water cloud model (IWCM) [4], [7]–[11], which models forest as a random volume with gaps and located above a ground surface. In the past, the IWCM has been used for biomass (or stem volume, closely related to biomass) estimation from both repeat-pass interferometric, C-band ERS-1/2 data [7]–[9], and single-pass interferometric, X-band TanDEM-X data [10], [11]. For ERS-1/2 data, the model included temporal decorrelation modeling, and biomass estimation relied primarily on the correlation between coherence and biomass, which was found to be the largest in frozen and windy conditions. For data from the single-pass SAR interferometer TanDEM-X, the temporal decorrelation can be neglected and biomass estimation relies primarily on the correlation between interferometric phase and biomass, provided that a terrain model is available. Although originally developed for the boreal forest, the IWCM has also proven itself useful with repeat-pass interferometric Envisat ASAR data over a tropical forest in India [12].

Compared with other models, such as the random volume over ground model [5] or the two-level model [6], the IWCM has a larger number of parameters in order to model both backscatter intensity and interferometric observables. Model parameters related to the electromagnetic properties of the forest (backscatter coefficients for ground and vegetation, canopy attenuation, zero-biomass coherence) are expected to be closely linked to the forest type and environmental parameters (moisture, temperature, precipitation, and snow cover), and are therefore treated as spatially invariant site and acquisition constants. Parameters describing forest properties (volume height and area-fill factor) are, however, assumed spatially variant. Moreover, the IWCM uses allometric equations to enforce an expected interdependence between forest parameters within the model. In [11], an approach to IWCM inversion using least-squares optimization and without the need for local training data was proposed for the first time.

In this letter, the IWCM inversion methods presented in [10] and [11] are further developed. Three cost functions are introduced, one for each observable, and a weighted sum of the three cost functions is minimized. The weights are calculated from the data using an iterative process and multiple

Manuscript received July 19, 2016; revised December 22, 2016 and February 20, 2017; accepted March 30, 2017. Date of publication May 29, 2017; date of current version June 22, 2017. This work was supported in part by the Swedish National Space Board and in part by the EU's 7th Framework Program under Grant 606971. (Corresponding author: Maciej J. Soja.)

The authors are with the Department of Space, Earth, and Environment Chalmers University of Technology, 412 96 Gothenburg, Sweden (e-mail: soja@chalmers.se; jan.askne@chalmers.se; lars.ulander@foi.se).

Color versions of one or more of the figures in this letter are available online at <http://ieeexplore.ieee.org>.

Digital Object Identifier 10.1109/LGRS.2017.2691355

random starting points are used to decrease the risk of finding local minima. The new inversion approach is used to study a large set of 87 VV-polarized TanDEM-X acquisitions over a boreal test site in northern Sweden. It is shown that the estimated model parameters are correlated with environmental parameters and thus carry physical significance.

II. INTERFEROMETRIC WATER CLOUD MODEL

In the IWCM, forest is represented by a random volume with gaps and located above a ground surface. Using z as the elevation coordinate and assuming that the ground is located at $z = 0$, the vertical backscatter intensity profile is defined as

$$\sigma(z) = \sigma_{\text{gr}}^0[(1 - \eta) + \eta e^{-ah}]\delta(z) + \sigma_{\text{veg}}^0 \eta \alpha e^{-\alpha(h-z)} \Theta(h-z) \Theta(z) \quad (1)$$

where $\delta(\cdot)$ is the Dirac delta function, $\Theta(\cdot)$ is the Heaviside step function, σ_{gr}^0 and σ_{veg}^0 are the backscatter coefficients of ground and vegetation, respectively, η is the area-fill factor, which is the fractional area covered by the volume, h is the volume height, and α is the two-way canopy attenuation coefficient.

A. Backscatter Modeling

Backscatter coefficient is the main SAR observable and it can be modeled by integrating $\sigma(z)$ in the vertical direction

$$\sigma^0 = \int_{-\infty}^{\infty} \sigma(z) dz = \eta [\sigma_{\text{gr}}^0 e^{-ah} + \sigma_{\text{veg}}^0 (1 - e^{-ah})] + (1 - \eta) \sigma_{\text{gr}}^0. \quad (2)$$

In (2), it is evident that there are three contributions to the total backscatter: backscatter from the ground passing through canopy gaps and modeled with $(1 - \eta) \sigma_{\text{gr}}^0$, backscatter from the ground attenuated by the canopy and modeled with $\eta \sigma_{\text{gr}}^0 e^{-ah}$, and backscatter from the canopy attenuated by the upper part of the canopy and modeled with $\eta \sigma_{\text{veg}}^0 (1 - e^{-ah})$.

B. Interferometric Modeling

The complex correlation coefficient is the main interferometric observable. It is a measure of similarity between two images. It typically has several contributions, including decorrelation due to thermal noise, system imperfections (ambiguities, quantization, processing, and phase noise), temporal changes, and spatial baseline.

Volume decorrelation is a spatial decorrelation effect carrying information about the vertical distribution of scatterers. It can be modeled as the Fourier transform of a normalized vertical backscatter intensity profile [13], which for (1) yields

$$\tilde{\gamma}_{\text{vol}}(k_z) = \frac{\int_{-\infty}^{\infty} \sigma(z) e^{ik_z z} dz}{\int_{-\infty}^{\infty} \sigma(z) dz} = \frac{\mu + \tilde{\gamma}_{\text{rv}}(k_z)}{\mu + 1} \quad (3)$$

where

$$\tilde{\gamma}_{\text{rv}}(k_z) = \frac{\alpha}{\alpha + ik_z} \frac{e^{ik_z h} - e^{-ah}}{1 - e^{-ah}} \quad (4)$$

$$\mu = \frac{\sigma_{\text{gr}}^0}{\sigma_{\text{veg}}^0} \frac{1 - \eta(1 - e^{-ah})}{\eta(1 - e^{-ah})} \quad (5)$$

are the random volume decorrelation and the ground-to-volume ratio, respectively, and k_z is the vertical wavenumber,

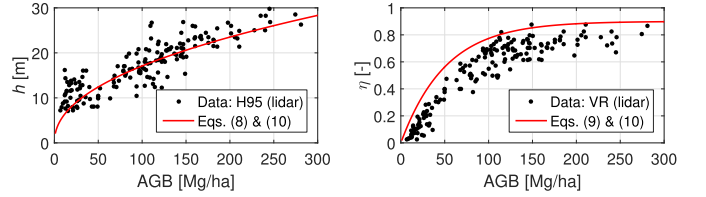


Fig. 1. Illustration of allometric equations (8)–(10). Data points show lidar metrics for the Remningstorp test site, situated in southern Sweden. Vegetation ratio is the fraction of laser returns classified as canopy returns. H95 is the 95th height percentile of laser returns classified as canopy returns.

which is the spatial frequency at which the interferometric measurement is made. A related quantity describing the interferometric setup is the height-of-ambiguity (HOA), which is the vertical height offset corresponding to a 2π -phase shift of the interferogram. HOA and k_z are related through: $\text{HOA} = 2\pi/k_z$.

In [10] and [11], decorrelation effects other than volume decorrelation are modeled using two real-valued decorrelation coefficients, one for the ground and one for the volume, which are found very similar for the studied single-pass interferometric, bistatic-mode TanDEM-X data. Therefore, in this letter, a single decorrelation term called zero-biomass coherence and denoted γ_0 will be used. For the TanDEM-X data studied in this letter, γ_0 is expected to be dominated by system and signal-to-noise ratio (SNR) decorrelation effects.

The two interferometric observables, coherence γ and interferometric height \tilde{h} (elevation of scattering phase center above ground), are modeled by the IWCM with the following expressions:

$$\gamma(k_z; \alpha, \rho, \gamma_0, h, \eta) = \gamma_0 |\tilde{\gamma}_{\text{vol}}(k_z; \alpha, \rho, h, \eta)| \quad (6)$$

$$\tilde{h}(k_z; \alpha, \rho, h, \eta) = \arg[\tilde{\gamma}_{\text{vol}}(k_z; \alpha, \rho, h, \eta)]/k_z \quad (7)$$

where $\rho = \sigma_{\text{gr}}^0/\sigma_{\text{veg}}^0$ is the ground-to-vegetation backscatter ratio, $|\cdot|$ is the absolute value operator, $\arg[\cdot]$ is the argument operator (including unwrapping), and where the dependence of the observables on model parameters has been expressed explicitly. Note that γ_0 only influences coherence and that ρ has been introduced to stress the fact that only the ratio between σ_{gr}^0 and σ_{veg}^0 affects the interferometric observables.

C. Allometric Functions

In [11], volume height h in meters (m), stem volume V in cubic meters per hectare (m^3/ha), and area-fill factor are linked to each other using the following two allometric equations:

$$h = h(V) = (2.44V)^{0.46} \quad (8)$$

$$\eta = \eta(V) = 0.9(1 - e^{-0.01V}). \quad (9)$$

Moreover, a third allometric equation is used to estimate stem volume V (in m^3/ha) from AGB (in Mg/ha):

$$V = V(\text{AGB}) = \text{AGB}/0.51. \quad (10)$$

Using (10) in (8) and (9), volume height and area-fill factor can be modeled from biomass. An illustration of these models is given in Fig. 1, where ALS data from the Remningstorp test site, situated in southern Sweden, are also shown. A motivation for models (8)–(10) can be found in [9] and [11].

D. Model Inversion

A cost function is defined for each of the three observables γ , \tilde{h} , and σ^0 as the mean squared difference between the modeled and observed values for each sample (e.g., stand or plot). For example, the cost function for γ is

$$J_\gamma(\mathbf{k}_z; \alpha, \rho, \gamma_0, \mathbf{AGB}) = \frac{1}{N} \sum_{i=1}^N [\gamma(k_{z,i}; \alpha, \rho, \gamma_0, h(V(\mathbf{AGB}_i)), \eta(V(\mathbf{AGB}_i))) - \gamma_i]^2 \quad (11)$$

where the individual samples are indexed with i , the total number of samples is N , and the vectors \mathbf{AGB} and \mathbf{k}_z contain biomass and vertical wavenumber values for all samples:

$$\mathbf{AGB} = [\mathbf{AGB}_1, \mathbf{AGB}_2, \dots, \mathbf{AGB}_i, \dots, \mathbf{AGB}_N]^T \quad (12)$$

$$\mathbf{k}_z = [k_{z,1}, k_{z,2}, \dots, k_{z,i}, \dots, k_{z,N}]^T. \quad (13)$$

Note that allometric functions (8)–(10) are used to express h and η in terms of AGB. Cost functions for backscatter intensity and interferometric height (J_σ and $J_{\tilde{h}}$) are defined accordingly.

The total cost function J is a weighted sum of the individual cost functions for the three observables:

$$J(\mathbf{k}_z; \alpha, \rho, \gamma_0, \sigma_{\text{veg}}^0, \mathbf{AGB}) = \frac{1}{s_\gamma^2} J_\gamma(\mathbf{k}_z; \alpha, \rho, \gamma_0, \mathbf{AGB}) + \frac{1}{s_{\tilde{h}}^2} J_{\tilde{h}}(\mathbf{k}_z; \alpha, \rho, \mathbf{AGB}) + \frac{1}{s_\sigma^2} J_\sigma(\alpha, \rho, \sigma_{\text{veg}}^0, \mathbf{AGB}) \quad (14)$$

where s_γ^2 , $s_{\tilde{h}}^2$, and s_σ^2 are weighting factors. The weighting factors both normalize the individual cost functions and compensate for different statistical properties of the modeled quantities.

IWCM inversion is done by finding such values for α , ρ , γ_0 , and σ_{veg}^0 and such vector of biomass estimates \mathbf{AGB} that the total cost function J is minimized. This requires finding suitable weighting factors. In this letter, an iterative, data-driven approach is proposed, as it shows a good tradeoff between simplicity and performance. In the first iteration, the variances of the corresponding observables are used as weighting factors. Thereafter, the cost function (14) is minimized, and first estimates of model parameters are obtained. A new estimate of the weighting factors is obtained by using the corresponding values of the individual cost functions with the first estimates of the model parameters. This process is repeated until model parameters become stable.

III. DATA

In this letter, data acquired over the boreal test site Krycklan (64° 14' N, 19° 46' E) [14], situated in northern Sweden, are used. The test site is hilly, with stand-level slopes reaching 19°, and it is dominated by Norway spruce and Scots pine.

A. Reference Data

All reference forest data have been acquired within the BioSAR 2008 campaign [14]. In this letter, 26 forest stands

with areas between 1.5 and 22 ha and unaltered between summer 2008 and September 2014 are used. They are a subset of the 31 stands used and described in [14] and [15] from which two stands have been removed due to harvesting activities done after summer 2008, one due to its small size, and two due to their location on a steep slope causing anomalous backscatter signatures. Biomass has been estimated using dedicated allometric equations and *in situ* measurements of stem diameter, species, and tree height done within 8–13, 10-m radius plots located within each stand. Growth has not been modeled and its effect is neglected in this letter.

As ground reference during InSAR processing, a 2 m × 2 m digital terrain model (DTM) acquired within a national laser scanning campaign conducted between 2009 and 2015 by Swedish Land Survey has been used. Meteorological data have been downloaded from the open database maintained by the Swedish Meteorological and Hydrological Institute. Three meteorological parameters are used in this letter: precipitation (both rain and melted snow/hail, in mm), measured at 6 A.M. UTC, snow depth (in cm), also measured at 6 A.M. UTC, and lowest temperature measured during the entire acquisition day (in °C).

B. TanDEM-X Data

Eighty-seven TanDEM-X [16] acquisitions made at VV-polarization on different occasions between June 2011 and September 2014 are used. 14 of these acquisitions have been made in the ascending mode (around 4 P.M. UTC), with an incidence angle of 41° and with low HOAs (13 acquisitions with HOAs between 36 m and 79 m). The remaining 73 acquisitions have been made in the descending mode (around 4 A.M. UTC), with an incidence angle of 44° and typically with higher HOAs, between 66 m and 277 m. Preprocessing done by the German Aerospace Center (DLR) included wavenumber shift filtering and coregistration. Interferometric processing was done using methods described in [6] and [15]. Stand-level estimates of σ^0 , γ , and \tilde{h} were computed as average values from the corresponding rasters of backscatter, coherence, and interferometric height, after applying a buffer zone of 5 m.

The cost function (11) was minimized using numerical optimization based on the trust-region-reflective algorithm, which is a modified Newton method for bounded problems, with good convergence and adaptive trust region size [17]. Parameters were constrained according to the following rules: $\alpha \in [0.01, 0.5] \text{ m}^{-1}$, $\rho \in [0.1, 3]$, $\gamma_0 \in [0.1, 1.2]$, $\sigma_{\text{veg}}^0 \in [0.1, 2]$, and $\mathbf{AGB} \in [0, 300] \text{ Mg/ha}$. The boundaries were chosen based on previous experience and (for biomass) *a priori* information about the forest type, and ensuring that the estimated parameter values never attained boundary values. Note that $\gamma_0 > 1$ was allowed on purpose, in order to be able to study the physical significance of γ_0 in this mathematical model. To minimize the risk of finding local minima, the minimization process was repeated for 100 different sets of initial values, randomly selected from uniform distributions with the aforementioned boundaries, and the solution with the lowest cost function J was selected. Four iterations were used to obtain reliable weighting factors. It was observed that the overall contribution of $J_{\tilde{h}}$ to J was higher compared

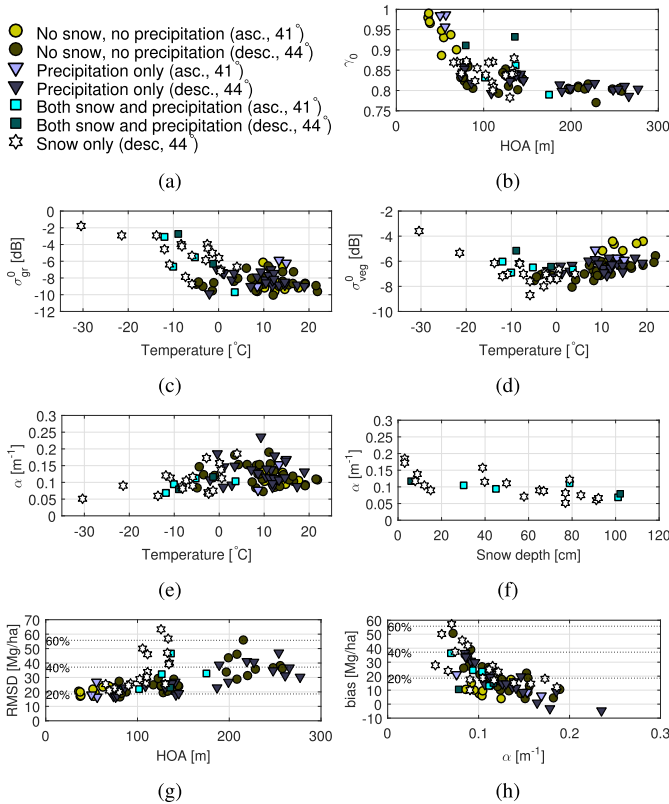


Fig. 2. Selected relations between estimated IWCM parameters, parameters related to system setup and meteorological conditions, and biomass estimation performance metrics. (a) Legend. (b) Zero-biomass coherence on HOA. (c) Ground backscatter on temperature. (d) Vegetation backscatter on temperature. (e) Canopy attenuation on temperature. (f) Canopy attenuation on snow depth. (g) Biomass RMSD on HOA. (h) Biomass bias on canopy attenuation.

to the other two individual cost functions, which indicated that the interferometric height model was more important than the other two models.

IV. RESULTS AND DISCUSSION

This section is divided into two parts. First, the dependence of the IWCM parameters γ_0 , σ_{gr}^0 , σ_{veg}^0 , and α on selected environmental and system parameters is studied. Thereafter, biomass estimation performance is studied.

A. Model Parameters

In Fig. 2(b), the dependence of γ_0 on HOA is shown. Zero-biomass coherence is close to 1 for HOAs around 40 m, and it decreases to roughly 0.8 as HOA increases beyond 150 m. The sensitivity of interferometric measurements to the exact vertical structure of the forest increases with decreasing HOA, as the signals scattered at different elevations within the canopy will have a larger difference in the interferometric phase at low HOAs. Since IWCM models forest canopy as a homogeneous random volume, this approximation is expected to be less valid at lower HOAs. Therefore, for large HOAs, γ_0 is expected to be dominated by system and SNR decorrelation. The value 0.8 agrees fairly well with modeling results presented in [16]. For small HOAs, γ_0 is expected to have a significant contribution from volume decorrelation effects not modeled accurately by the

random volume approximation. Since γ_0 is significantly higher than 0.8 at low HOA, the modeled volumetric coherence appears to be too low and it requires compensation from γ_0 for the model to agree with the observables.

In Fig. 2(c) and (d), the dependence of σ_{gr}^0 and σ_{veg}^0 on temperature is shown. For acquisitions made over a snow-covered scene, ground backscatter coefficient σ_{gr}^0 decreases with increasing temperature, see Fig. 2(c), from a little above -3 dB for temperatures below -20 °C down to between -6 dB and -10 dB for temperatures above 0 °C. A similar observation can be made for vegetation backscatter coefficient σ_{veg}^0 [see Fig. 2(d)], which decreases from just above -4 dB for one acquisition made at a temperature around -30 °C down to between -6 dB and -8 dB for temperatures between -5 °C and 5 °C. Decreasing backscatter coefficient can be attributed to a combination of decreasing volume scattering in dry snow at low temperatures when snow thickness decreases, and increasing absorption and forward scattering in smooth, wet snow. This applies to snow located both on the ground and in tree canopies.

For the snow-free cases, σ_{gr}^0 appears to be uncorrelated with temperature. However, the attained values vary the most (between -10 dB and -6 dB) for temperatures between 0 °C and 15 °C, and less outside that interval (between -10 dB and -8 dB), which may be due to largest soil moisture variations in that interval. At the same time, σ_{veg}^0 clearly increases up to almost -4 dB for temperatures above 10 °C, which can be attributed to increasing moisture in tree canopies.

Note also that the acquisitions with the highest σ_{veg}^0 observed for temperatures around and above 10 °C were made in the ascending mode, i.e., around 4 P.M. local time. Since the temperatures shown on the x -axis are the minimal temperatures measured on the day of the acquisition, current temperatures for the ascending-mode acquisitions may have been higher, which should make the observed trend even more prominent.

In Fig. 2(e), the dependence of α on temperature is shown. There is a large variance in α , especially for the acquisitions made at temperatures above 0 °C. For acquisitions made over snow-covered forest, α seems to decrease slightly with decreasing temperature. In Fig. 2(f), α is plotted against snow depth for acquisitions made when snow cover was present. A weak trend can be observed, which implies that increasing snow cover causes a decreasing canopy attenuation α . This observation will be discussed in the following section.

B. Biomass Estimation Performance

In Fig. 2(g), root-mean-square difference (RMSD) between the estimated and reference biomass values for the different acquisitions is plotted against HOA. It can be observed that for all 43 acquisitions made in snow-free conditions and at HOAs below 150 m the stand-level RMSD for biomass is between 18% and 32% of the mean biomass of 94 Mg/ha, which is in line with other results presented in the literature (see [10], [11], [15] and references therein). For approximately half of the acquisitions of snow-covered forest and for most acquisitions made at HOAs above 150 m, the RMSD is well above 35%. As the Pearson correlation coefficient r is

very high, between 0.81 and 0.93 for all acquisitions, the large RMSD is mainly due to a significant bias.

The model parameter most directly affecting biomass estimation is α , which describes canopy attenuation. In (2), (4), and (5), the product of α and h is found in e^{-ah} , which models canopy attenuation. Additionally, in (4), α can be found in $(\alpha/(\alpha + ik_z))$, whereas h can be found in $e^{ik_z h}$. As HOA increases, k_z decreases and the two terms $\alpha/(\alpha + ik_z)$ and $e^{ik_z h}$ lose their sensitivity to α and h respectively. Therefore, for large HOAs, e^{-ah} will be the most important term containing α and h , and separation of the space-invariant parameter α from the space-variant parameter h will become increasingly difficult. Moreover, height measurement sensitivity decreases with increasing HOA. These effects will cause biases in estimates of both α and h , and thus also AGB. An overestimation of biomass will therefore be connected to underestimation of α . This reasoning is also supported by observations in experimental data. In Fig. 2(h), the observed bias is plotted against the estimated α for the 87 acquisitions studied in this letter, and a clear correlation can be observed.

For approximately half of the acquisitions made over a snow-covered scene, the RMSD is high due to low α values. However, for most of these cases, HOA is low, meaning that the aforementioned effect cannot be held responsible for the poor biomass estimation. Instead, possible causes for this may be: effects not included or modeled accurately by the model (for example, phase shifts introduced in the snow) and inaccuracies in the allometric formulas due to winter conditions. In any case, the solution of this problem is left for future studies.

The estimated model parameters and biomass performance were also studied against time and precipitation, but no trends were observed. This implies that neither precipitation nor growth seems to have a significant influence on IWCM parameters, although a more thorough analysis is needed before a final conclusion can be drawn.

V. CONCLUSION

This letter introduces a new approach to IWCM inversion of TanDEM-X data over a boreal forest. IWCM inversion is carried out for 87 VV-polarized TanDEM-X acquisitions made with HOAs between 36 m and 277 m over the boreal test site Krycklan, situated in northern Sweden. IWCM parameters describing ground and vegetation backscatter coefficients (σ_{gr}^0 and σ_{veg}^0 , respectively) and canopy attenuation (α) are found correlated with temperature and snow cover, whereas zero-biomass coherence (γ_0) is found correlated with HOA. Possible explanations for the observed trends are also given.

Biomass estimation performance is evaluated, and it is observed that for all 43 acquisitions made in snow-free conditions and at HOAs between 36 m and 150 m, the stand-level RMSD is between 18% and 32% of the mean biomass of 94 Mg/ha, which is in line with other results presented in the literature. For all 87 acquisitions, the correlation between the estimated and reference biomass values is high, with r between 0.81 and 0.93. It is found that biomass estimates are biased for acquisitions made at high HOAs as well as for some

acquisitions made over snow-covered forest, and further work is advised before reliable biomass estimation can be obtained for these cases.

ACKNOWLEDGMENT

The authors would like to thank DLR for the TanDEM-X data, the Swedish Land Survey for the DTM data, SMHI for the meteorological data, the European Space Agency for the BioSAR 2008 data, and the anonymous reviewers for their invaluable comments.

REFERENCES

- [1] B. Koch, "Status and future of laser scanning, synthetic aperture radar and hyperspectral remote sensing data for forest biomass assessment," *ISPRS J. Photogramm. Remote Sens.*, vol. 65, no. 6, pp. 581–590, 2010. [Online]. Available: <http://www.sciencedirect.com/science/article/pii/S0924271610000845>
- [2] L. M. H. Ulander and J. I. H. Askne, "Repeat-pass SAR interferometry over forested terrain," *IEEE Trans. Geosci. Remote Sens.*, vol. 33, no. 2, pp. 331–340, Mar. 1995.
- [3] R. N. Treuhaft, S. N. Madsen, M. Moghaddam, and J. J. van Zyl, "Vegetation characteristics and underlying topography from interferometric radar," *Radio Sci.*, vol. 31, no. 6, pp. 1449–1485, 1996.
- [4] J. I. H. Askne, P. B. G. Dammert, L. M. H. Ulander, and G. Smith, "C-band repeat-pass interferometric SAR observations of the forest," *IEEE Trans. Geosci. Remote Sens.*, vol. 35, no. 1, pp. 25–35, Jan. 1997.
- [5] S. R. Cloude and K. P. Papathanassiou, "Polarimetric SAR interferometry," *IEEE Trans. Geosci. Remote Sens.*, vol. 36, no. 5, pp. 1551–1565, Sep. 1998.
- [6] M. J. Soja, H. Persson, and L. M. H. Ulander, "Estimation of forest height and canopy density from a single InSAR correlation coefficient," *IEEE Geosci. Remote Sens. Lett.*, vol. 12, no. 3, pp. 646–650, Mar. 2015.
- [7] M. Santoro, J. I. H. Askne, G. Smith, and J. E. S. Fransson, "Stem volume retrieval in boreal forests from ERS-1/2 interferometry," *Remote Sens. Environ.*, vol. 81, no. 1, pp. 19–35, 2002.
- [8] J. I. H. Askne, M. Santoro, G. Smith, and J. E. S. Fransson, "Multitemporal repeat-pass SAR interferometry of boreal forests," *IEEE Trans. Geosci. Remote Sens.*, vol. 41, no. 7, pp. 1540–1550, Jul. 2003.
- [9] J. I. H. Askne and M. Santoro, "Experiences in boreal forest stem volume estimation from multitemporal C-band InSAR," in *Recent Interferometry Applications in Topography and Astronomy*. Rijeka, Croatia: InTech, 2012.
- [10] J. I. H. Askne, J. E. S. Fransson, M. Santoro, M. J. Soja, and L. M. H. Ulander, "Model-based biomass estimation of a hemi-boreal forest from multitemporal TanDEM-X acquisitions," *Remote Sens.*, vol. 5, no. 11, pp. 5574–5597, 2013.
- [11] J. I. H. Askne and M. Santoro, "On the estimation of boreal forest biomass from TanDEM-X data without training samples," *IEEE Geosci. Remote Sens. Lett.*, vol. 12, no. 4, pp. 771–775, Apr. 2015.
- [12] S. Kumar, U. Pandey, S. P. Kushwaha, R. S. Chatterjee, and W. Bijker, "Aboveground biomass estimation of tropical forest from Envisat advanced synthetic aperture radar data using modeling approach," *J. Appl. Remote Sens.*, vol. 6, no. 1, p. 063588, 2012.
- [13] H. A. Zebker and J. Villasenor, "Decorrelation in interferometric radar echoes," *IEEE Trans. Geosci. Remote Sens.*, vol. 30, no. 5, pp. 950–959, Sep. 1992.
- [14] I. Hajnsek *et al.*, "BioSAR 2008 technical assistance for the development of airborne SAR and geophysical measurements during the BioSAR 2008 experiment: Final report—BioSAR campaign," ESA, Paris, France, Tech. Rep., 2009.
- [15] M. J. Soja, H. J. Persson, and L. M. H. Ulander, "Estimation of forest biomass from two-level model inversion of single-pass InSAR data," *IEEE Trans. Geosci. Remote Sens.*, vol. 53, no. 9, pp. 5083–5099, Sep. 2015.
- [16] G. Krieger *et al.*, "TanDEM-X: A satellite formation for high-resolution SAR interferometry," *IEEE Trans. Geosci. Remote Sens.*, vol. 45, no. 11, pp. 3317–3341, Nov. 2007.
- [17] T. F. Coleman and Y. Li, "An interior trust region approach for nonlinear minimization subject to bounds," *SIAM J. Optim.*, vol. 6, no. 2, pp. 418–445, 1996.